A Novel Gene Expression Profile in Lymphatics Associated with Tumor Growth and Nodal Metastasis

Steven Clasper,[1] Daniel Royston,[1] Dilair Baban,[2] Yihai Cao,[3] Stephan Ewers,[4] Stefan Butz,[4] Dietmar Vestweber,[4] and David G. Jackson[1]

[1]MRC Human Immunology Unit, Weatherall Institute of Molecular Medicine, John Radcliffe Hospital; [2]MRC Functional Genetics Unit, Department of Human Anatomy and Genetics, Oxford, United Kingdom; [3]Microbiology and Tumor Biology Centre, Karolinska Institute, Stockholm, Sweden; and [4]Max Planck Institute for Molecular Biomedicine, Münster, Germany

Abstract

Invasion of lymphatic vessels is a key step in the metastasis of primary tumors to draining lymph nodes. Although the process is enhanced by tumor lymphangiogenesis, it is unclear whether this is a consequence of increased lymphatic vessel number, altered lymphatic vessel properties, or both. Here we have addressed the question by comparing the RNA profiles of primary lymphatic endothelial cells (LEC) isolated from the vasculature of normal tissue and from highly metastatic T-241/vascular endothelial growth factor (VEGF)-C fibrosarcomas implanted in C57BL/6 mice. Our findings reveal significant differences in expression of some 792 genes (i.e., ≥2-fold up- or down-regulated, $P \leq 0.05$) that code for a variety of proteins including components of endothelial junctions, subendothelial matrix, and vessel growth/patterning. The tumor LEC profile, validated by immunohistochemical staining, is distinct from that of normal, inflammatory cytokine, or mitogen-activated LEC, characterized by elevated expression of such functionally significant molecules as the tight junction regulatory protein endothelial specific adhesion molecule (ESAM), the transforming growth factor-β coreceptor Endoglin (CD105), the angiogenesis-associated leptin receptor, and the immunoinhibitory receptor CD200, and reduced expression of subendothelial matrix proteins including collagens, fibrillin, and biglycan. Moreover, we show similar induction of ESAM, Endoglin, and leptin receptor within tumor lymphatics in a series of human head and neck and colorectal carcinomas, and uncover a dramatic correlation between ESAM expression and nodal metastasis that identifies this marker as a possible prognostic indicator. These findings reveal a remarkable degree of phenotypic plasticity in cancer lymphatics and provide new insight into the processes of lymphatic invasion and lymph node metastasis. [Cancer Res 2008;68(18):7293–303]

Introduction

Early lymph node metastasis is a common clinical finding in many human cancers, and one that is associated both with aggressive disease and poor prognosis. Clearly, treatments to specifically block dissemination through the lymphatic network would be desirable either as independent therapies or as adjuncts to existing chemotherapy (1). However, the ability to develop such approaches is currently handicapped by poor understanding of lymphatic vessel molecular biology and ignorance of the molecular interactions that occur between migrating cells and lymphatic vessel endothelium (see ref. 2 for recent review). This contrasts with the blood vascular system, where at least the basic mechanisms regulating vessel wall transmigration have been well studied and extensively characterized (3).

The target vessels for invasion by lymph-metastasizing tumor cells include preexisting tissue lymphatics abutting the tumor mass either through coincidence or mutual chemoattraction (4), as well as new lymphatic vessels that proliferate either within or around the tumor as a result of lymphangiogenesis (5, 6). The latter process is regulated primarily by the lymphangiogenic growth factors VEGF-C and VEGF-D generated by tumor cells or by host cells including tissue macrophages (6). Indeed, recent reports show an association between elevated lymphatic vessel density and either nodal metastasis or reduced 5-year survival in several human cancers (2). Moreover, in animal tumor models, the induction of lymphangiogenesis by engineered overexpression of VEGF-C/D can be sufficient to trigger invasion and lymph node metastasis (7–9). Nevertheless, it remains controversial as to whether this metastasis-enhancing effect results simply from an increase in the number of target vessels due to mitogenesis or if other properties of the newly dividing tumor lymphatics, such as increased permeability, increased lymph flow, or specific changes in lymphatic surface phenotype, predispose them to invasion by tumor (10–13).

In the tumor blood vasculature, recent RNA profiling of immunoselected human tumor endothelial cells using Sequential Analysis of Gene Expression analysis has revealed significant alterations in gene expression that seem to correlate with propensity for hematogenous metastasis (14). This has led to the identification of a number of candidate tumor endothelial markers that are mechanistically implicated in tumor metastasis (15, 16), some of which are currently being evaluated for prognostic and therapeutic targeting applications (14, 17). Thus far, no similar studies have been reported for tumor lymphatics and there is currently no prospect of corresponding markers for the prediction of lymphogenic metastasis.

Here we present the first comparative profiling of normal and tumor-associated lymphatic endothelial cells (LEC) isolated from lymph node metastasizing T-241/VEGF-C mouse fibrosarcomas, using combined GeneChip microarray and immunohistochemical analyses. We reveal an expression pattern in metastasizing tumor LEC distinct from that of nonmetastasizing tumor LEC, normal dermal LEC, or mitogen (VEGF-C)–activated or inflammation-activated LEC, particularly with respect to molecules associated

Note: Supplementary data for this article are available at Cancer Research Online (http://cancerres.aacrjournals.org/).

S. Clasper and D. Royston contributed equally.

Requests for reprints: David G. Jackson, MRC Human Immunology Unit, Weatherall Institute of Molecular Medicine, John Radcliffe Hospital, Headington, Oxford OX3 9DS, United Kingdom. Phone: 44-1865-222313; Fax: 44-1865-222502; E-mail: djackson@hammer.imm.ox.ac.uk.

doi:10.1158/0008-5472.CAN-07-6506

with interendothelial junction and subendothelial matrix integrity. Importantly, we validate key aspects of these findings in human cancers by showing selective expression in tumor lymphatics of the endothelial specific adhesion molecule (ESAM), the transforming growth factor-β (TGFβ) coreceptor Endoglin, and the angiogenesis associated leptin receptor (leptin-R). Lastly, we present new evidence of a strong association between ESAM expression and lymph node metastasis in a series of head and neck squamous cell carcinomas (HNSCC) and colorectal carcinomas, indicating the possible value of this marker as a prognostic indicator for disseminated disease. Together these findings identify a pool of novel candidate biomarkers for tumor lymphatics whose evaluation should provide powerful insight into the mechanisms of lymphogenic metastasis.

Materials and Methods

Cells

Murine T241 fibrosarcoma cells transfected with green fluorescent protein (GFP) and either empty vector (nonmetastatic T-241 control) or a construct encoding human recombinant VEGF-C (T-241/VEGF-C/GFP) were cultured in RPMI 1640 supplemented with 10% FCS as described previously (18). Primary mouse dermal LEC and T-241 fibrosarcoma LEC (see below) were grown in gelatin-coated tissue culture flasks in EGM-2 medium (Clonetics).

Antibodies

Antibodies to human and mouse LYVE-1 (19) and mouse ESAM (20) have been described previously. Polyclonal goat anti-human ESAM, goat anti-human LYVE-1, and goat anti-mouse VEGF receptor 3 (VEGFR3) antibodies were from R&D Systems Europe; mouse anti-human Endoglin was from DAKO; polyclonal rabbit anti-human leptin-R antibodies were from Abcam; rat anti-mouse CD31, Endoglin, and MECA-32 monoclonal antibodies were from BD Pharmingen; rabbit anti-Prox1 was from Research Diagnostics Inc.; goat anti-mouse biglycan was from Santa Cruz Biotechnology; and rabbit anti-human CD200 was from Serotec UK. Rabbit anti-mouse podoplanin and rat anti-mouse CD200 were kind gifts from D. Kerjaschki and N. Barclay, respectively. Alexa Fluor 488 and 568/594 conjugates were from Invitrogen.

Mouse Fibrosarcoma Lymphatic Metastasis Model

T241/VEGF-C/GFP fibrosarcoma cells (2×10^6/mL) in sterile PBS (pH 7.5) were injected s.c. (100 μL) to the right mid-dorsum of 8-wk-old female C57BL/6 mice. After the 7th day, mice were checked regularly for primary tumor growth and sacrificed before the tumor exceeded ethical limits (generally day 14). Metastasis to the draining axillary lymph node was confirmed postmortem after dissection either by visualization of GFP-containing tumor cells within frozen sections of lymph nodes or by *in vitro* outgrowth of GFP-containing tumor cells from individual nodes.

Immunomagnetic Isolation of Fibrosarcoma and Normal Murine LEC

Normal dermal LEC were isolated from the tail skin of 8-wk-old female C57BL/6 mice (8–12 mice per preparation). Briefly, skin was incubated at 4°C overnight in PBS containing 2 mg/mL dispase to remove epidermis, and endothelial cells were released from dermis by scraping into a Petri dish containing EBM-2 medium. The mixed dermal cell populations were collected by centrifugation and cultured in gelatin-coated flasks (24 h) before detachment with Accutase; purification of LEC was done by immunomagnetic selection with rabbit anti-mouse LYVE-1 antibodies and goat anti-rabbit MACS beads according to the manufacturer's instructions. LEC were then expanded in culture (3–4 d) in six-well multiwell dishes (total of 1×10^6–1.5×10^6 cells per preparation) before isolation of RNA and phenotypic analysis.

For isolation of LEC from T241/VEGF-C/GFP fibrosarcomas, primary tumors from mice exhibiting nodal metastases were first minced and incubated (1 h, 37°C) with shaking in PBS (pH 7.5) containing collagenase (1 mg/mL), elastase (0.1 mg/mL), hyaluronidase (2 mg/mL), and DNase (0.1 mg/mL). The dispersed tissue was then filtered and washed by centrifugation/resuspension in EGM-2 medium before culture in gelatin-coated flasks. The majority of contaminating tumor cells were then removed by selective detachment with PBS, 5 mmol/L EDTA before lifting of the more strongly adherent LEC with Accutase, purification by LYVE-1 immunomagnetic bead selection, and expansion in culture (3–4 d; total yield, 0.5×10^6–1×10^6 cells) for RNA isolation and phenotyping as described for dermal LEC.

Phenotyping of LEC by Immunofluorescence Microscopy and Flow Cytometry

For single/double immunofluorescent staining of cultured LEC, primary antibodies were applied in PBS supplemented with FCS (5%, v/v), typically at 10 μg/mL, and incubated at 25°C for 30 min. Cells were washed briefly with PBS (pH 7.5) before incubation with Alexa Fluor secondary antibodies at 10 μg/mL in PBS-5% FCS. Samples were fixed in 2% formaldehyde-PBS (v/v) for 10 min, mounted in VectaShield-4′,6-diamidino-2-phenylindole (VectaShield-DAPI; Vector Laboratories Inc.), and then viewed under a Zeiss Axiovert fluorescence microscope and captured with a Hamamatsu Orca digital video camera and ImproVision Openlab software.

For flow cytometry, cultured LEC were lifted with Accutase (PAA Laboratories), suspended in incubation buffer (PBS-5% FCS, 0.1% azide), and incubated (30 min, 5°C) with primary antibody followed by washing and reincubation (30 min, 5°C) with the appropriate Alexa Fluor 488 goat conjugate before analysis on a FACscalibur flow cytometer using CellQuest software.

Affymetrix GeneChip Microarray Analysis

Total cellular RNA was isolated (RNeasy, Qiagen) from freshly derived primary LEC (3× independent normal LEC cultures and 3× T-241/VEGF-C tumor LEC cultures; 0.5×10^6–1×10^6 cells per culture) before analysis and quantitation with NanoDrop ND-1000 and an Agilent Bioanalyzer 2100 (Agilent). cRNA probe preparation (50 ng input RNA) and hybridization to high-density oligonucleotide mouse MOE430_2.0 arrays (Affymetrix) were carried out using procedures described in the GeneChip expression technical manual (Affymetrix) as previously reported (19). Following hybridization, arrays were processed using a GeneChip Fluidics Station 450 according to the recommended protocols (EukGE-WS2v5, Affymetrix) of double staining and posthybridizations washes. Fluorescent images were captured using gene Array Scanner 3000 (Affymetrix). All experiments were designed and all information was compiled in compliance with MIAME (21) guidelines to facilitate correct interpretation and independent verification of microarray data.

Data Analysis and Bioinformatics

Gene transcript levels were determined from data image files using algorithms in Gene Chip Operating Software (GCOS1.2, Affymetrix) with global scaling. Data analysis was done using Data Mining Tool (DMT 3.1, Affymetrix) and GeneSpring 7.2 (Silicon Genetics). The Robust Multiarray Average expression measurement was also used with help of probe sequence (GC content) information (GC Robust Multiarray Average; refs. 22, 23) as implemented in BioConductor R statistics.[5] Cell Intensity files (.CEL) were processed into expression values for all the 45,101 probe sets (transcripts) on each array and following the respective normalization step. Differentially expressed genes were selected if they passed Welch's *t* test and parametric test (variance not assumed equal, $P < 0.05$) and showed at least 2-fold changes between normal and tumor-associated LEC. Differentially expressed genes are classified according to the Gene Ontology functional category and GenMAPP and KEGG pathways. The array data have been deposited in the National Center for Biotechnology Information (NCBI) Gene Expression Omnibus (GEO)[6] and are accessible through GEO Series accession no. GSE6255.

[5] http://www.bioconductor.org
[6] http://www.ncbi.nlm.nih.gov/geo/

Semiquantitative PCR

cDNA was prepared from total RNA by reverse transcription using oligo dT primers. PCR primer sequences were obtained from PrimerBank (24). Reaction cycle numbers for amplification were optimized to ensure that the reaction mix was sampled during the log phase.

Validation of Affymetrix Array Analyses by Immunofluorescence Microscopy and Immunohistochemistry

Mouse tissues. Thin frozen sections of normal mouse skin, T-241 control, or T-241/VEGF-C tumor tissue were prepared by freezing in optimum cutting temperature embedding medium (purchased from R.A Lamb Laboratory Supplies) before cutting 8-μm or thinner sections by cryostat. Nonspecific binding was blocked by incubation with 10% goat serum in PBS (pH 7.5) before application of primary antibodies (10 μg/mL) in 5% FCS in PBS followed by appropriate Alexa Fluor 488/586 conjugates (10 μg/mL). Sections were mounted in VectaShield-DAPI and images captured as above.

Human tissues. A panel of 28 cases of HNSCC, 28 cases of primary colorectal carcinoma, and 2 cases each of cutaneous melanoma and primary breast ductal adenocarcinoma (grade 2) was assembled by random selection from the histopathology database at the John Radcliffe Hospital Pathology Department, with full professional approval and in accordance with local ethic committee guidelines.

Colorectal carcinoma cases varying in stage from T_2 to T_4 (equal numbers) were divided into two groups of 14 cases based on the presence or absence of lymph node metastasis at time of resection. Lymph node metastasis was defined as histologic identification of tumor cells in regional or distant lymph nodes that were free from local extension by primary tumor; only cases where evidence of lymph node involvement was confirmed by subsequent histologic assessment were included. Due to size limitations with HNSCC sections, lymph node metastasizing and nonmetastasizing tumors were approximately matched by maximum microscopic dimension and grade rather than tumor stage. Serial sections (4 μm) were cut onto silanized glass slides before dewaxing, rehydration, and microwave retrieval as described previously (5). Sections were then stained with antibodies to ESAM (1 μg/mL), Endoglin (0.6 μg/mL), or leptin-R (0.5 μg/mL) and developed using the peroxidase-catalyzed biotin-tyramide signal amplification procedure (CSA system, DakoCytomation) for light microscopy or detection with streptavidin Alexa Fluor 488, followed by staining with goat anti-human LYVE-1/donkey anti-goat Alexa Fluor 586 or mouse anti-human LYVE-1/goat anti-mouse Alexa Fluor 586 and mounting in VectaShield-DAPI for fluorescence microscopy.

Vessels doubly positive for Endoglin and LYVE-1, ESAM and LYVE-1, or leptin-R and LYVE-1 were scored as tumoral if present within the main tumor mass or a perimeter zone of one ×10 field of magnification (3.14 mm^2) from the main tumor edge. Marginal tissue was defined as normal tissue (with no significant inflammation or fibrosis) >1 mm from the outer margin of this perimeter zone. For Endoglin/LYVE-1 double-positive vessels, five fields of view containing lymphatic vessel hotspots (each at ×20 magnification = 0.79 mm^2) were assessed for vessel counts in tumoral and marginal tissue in each case. For ESAM/LYVE-1 and leptin-R/LYVE-1 double-positive vessels, the total number of vessels within 10 random fields (×10 magnification) was counted. In some experiments, vessels were also scored according to staining intensity and pattern as either weak (granular patchy staining) or strong (bright continuous or discontinuous wall staining).

Statistics

Statistical analyses were carried out for the association between Endoglin, ESAM, and leptin-R positive lymphatic vessel number and tumoral/normal marginal location and for Endoglin expression level with tumoral/normal marginal location within the group of 28 HNSCC and colorectal cancer cases using the *t* test. Similar analyses were also carried out for the association between Endoglin-, ESAM-, and leptin-positive vessel number and presence or absence of lymph node metastasis.

Results

Isolation and characterization of LEC derived from murine T-241/VEGF-C tumors. As a model system to study the effects of tumor environment on LEC phenotype, we used the GFP-transfected T241/VEGF-C tumor line (18) that consistently forms lymph node metastasizing fibrosarcomas when implanted in the dermis of C57BL/6 mice, characterized by formation of extensive intratumoral and peritumoral LYVE-1^{+ve}/Podoplanin^{+ve}/PROX-1^{+ve} lymphatic vessels (see Supplementary Fig. S1). For the analyses, we isolated LEC both from T-241/VEGF-C fibrosarcomas harvested 12 to 14 days after initial implantation (tumor LEC) and from normal dermis (normal LEC) using immunomagnetic bead selection with affinity-purified LYVE-1 antisera. The resulting populations in each case coexpressed the lymphatic markers LYVE-1, podoplanin, VEGFR3, and Prox-1, together with the pan-endothelial marker CD31, indicating their authentic LEC phenotype (Fig. 1*A* and *B*). As expected, the cultures displayed some heterogeneity in LYVE-1 expression—a characteristic shared by the receptor in intact tissue lymphatics (see, e.g., Supplementary Figs. S1, S3, and S4) that is partly due to regulated LYVE-1 uptake and lysosomal degradation (25). Overall purity was estimated to be in excess of 98% as assessed by fluorescence-activated cell sorting (FACS) analysis for either podoplanin or LYVE-1, indicating the absence of any significant contamination with stromal tissue or tumor cells. Furthermore, normal dermal and T-241/VEGF-C tumor LEC were uniformly negative for MECA-32, a murine blood vascular endothelial marker (see Supplementary Fig. S1 and data not shown), indicating the absence of contaminating blood vascular endothelial cells. Lastly, the three-dimensional culture properties of the two LEC populations were similar insofar as both showed identical capacities for tube formation in Matrigel (data not shown).

Metastatic T-241/VEGF-C tumor LEC have a distinct transcriptional profile. Having confirmed the authenticity of the LEC populations by immunofluorescence microscopy and flow cytometry, we next compared their transcriptional profiles by generating cRNA probes for hybridization to Affymetrix mouse 430 GeneChip arrays. The results (Fig. 1*C*; NCBI GEO database accession GSE6255) revealed differential expression of some 792 genes including 271 that were up-regulated and 521 that were down-regulated in T-241/VEGF-C tumor compared with normal dermal LEC by ≥2-fold ($P \leq 0.05$). Based on potential relevance to metastasis, we focused initially on transcripts associated with cell-cell adhesion and endothelial junction formation, as well as others encoding extracellular matrix components and vessel growth/patterning factors, yielding the representative panel shown in Table 1. The changes in levels of 15 transcripts chosen from this panel were independently confirmed by a limited cycle semiquantitative reverse transcriptase PCR (Supplementary Fig. S2) and in selected examples by comparative immunohistochemical staining of frozen tissue (Fig. 2).

Changes in endothelial junction and adhesion molecules. Most notably among endothelial cell adhesion molecules, the tight junction–associated molecule JAM-A (*F11r*) and the closely related molecules Coxsackie adenovirus receptor (*Cxadr*), ESAM (*Esam1*), the nectin family adherens junction component CD112, and the adhesion-associated α actinin-binding protein Ajuba showed up-regulation in tumor LEC, whereas JAM-B (VE-JAM, *Jam-2*) was down-regulated. Given that these molecules mediate steps in the transmigration of discrete leukocyte populations across blood and

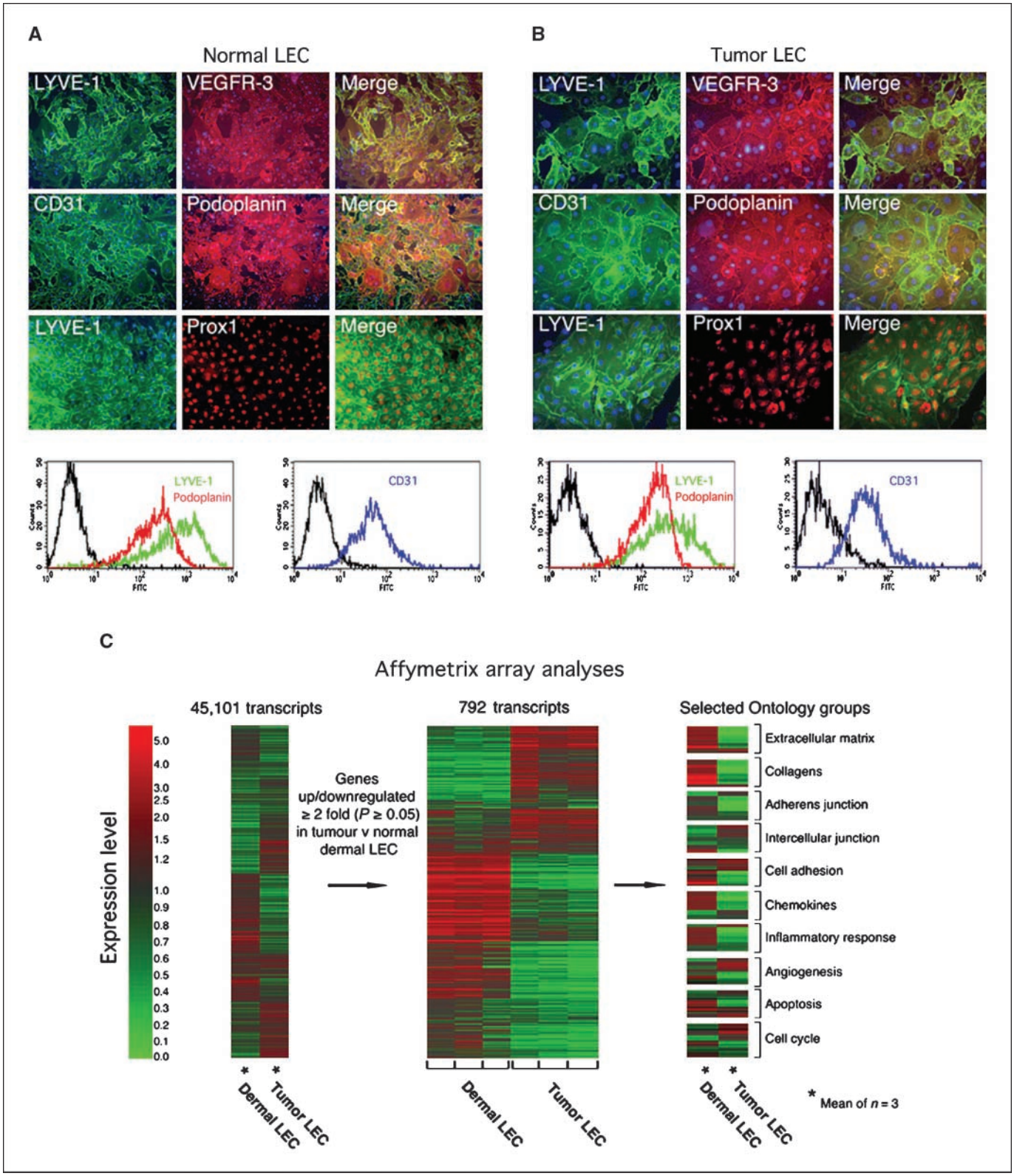

Figure 1. Characterization and transcriptional profiling of mouse T-241/VEGF-C fibrosarcoma LEC and normal dermal LEC. Primary cultures of LYVE-1 immunomagnetic bead–selected normal dermal LEC (*A*) and T241/VEGF-C fibrosarcoma LEC (*B*) are shown dual stained for LYVE-1 and either VEGFR3 or Prox-1, or for the pan-endothelial marker CD31 and podoplanin, followed by Alexa 488 (*green*) or Alexa 568 (*red*) conjugates as indicated. Original magnification, ×20. Representative FACS histograms show expression levels of LYVE-1 (*green*), podoplanin (*red*), CD31 (*blue*), and irrelevant immunoglobulin control (*black*). Variation in LYVE-1 expression reflects heterogeneity seen in intact tissues (see text and Supplementary Fig. S1). *C,* Affymetrix mouse 430 GeneChip array analyses showing the 792 transcripts up- or down-regulated >2-fold ($P \leq 0.05$) in T241/VEGF-C (*Tumor*) LEC compared with normal (*Dermal*) LEC. Data are represented as heatmaps using GeneTree software. Expression levels relative to the mean chip value are graded from red (above average) through green (below average) according to the calibration scale shown on the left.

Table 1. Genes up-regulated or down-regulated in T241/VEGF-C–derived LEC compared with normal skin–derived LEC ($P \leq 0.05$)

Affymetrix probe ID	Transcript	Gene	Fold change
Cell adhesion and junctional proteins			
1453282_at	Coxsackie adenovirus receptor	*Cxadr*	+5.3
1460356_at	Endothelial specific adhesion molecule	*Esam1*	+3.9
1421344_a_at	Ajuba	*Jub*	+2.9
1424595_at	Junctional adhesion molecule A	*F11r*	+2.6
1417703_at	CD112	*Pvrl2*	+2.2
1450757_at	Cadherin 11	*Cdh11*	−108
1449244_at	N-Cadherin	*Cdh2*	−78
1428547_at	CD73	*N5te*	−13
1436568_at	Junctional adhesion molecule B	*Jam2*	−9.5
Extracellular matrix			
1416342_at	Tenascin-C	*Tnc*	+5.3
1450857_a_at	Procollagen I α2	*Col1a2*	−954
1448323_a_at	Biglycan	*Bgn*	−625
1427883_a_at	Procollagen III α1	*Col3a1*	−315
1451978_at	Lysyl oxidase like 1	*Loxl1*	−121
1416121_at	Lysyl oxidase	*Lox*	−73
1426285_at	Laminin α2	*Lama2*	−65
1426947_x_at	Procollagen VI α2	*Col6a2*	−61
1451527_at	Procollagen C-endopeptidase enhancer 2	*Pcolce2*	−44
1448590_at	Procollagen VI α1	*Col6a1*	−41
1437165_at	Procollagen C-endopeptidase enhancer	*Pcolce*	−37
1416740_at	Procollagen V α1	*Col5a1*	−18
1418061_at	Latent transforming growth factor β binding protein 2	*Ltbp2*	−18
1427257_at	Versican	*Cspg2*	−16
1435264_at	Elastin microfibril interfacer 2	*Emilin2*	−14
1424131_at	Procollagen VI α3	*Col6a3*	−10
1448870_at	Latent transforming growth factor β binding protein 1	*Ltbp1*	−3.6
1425896_at	Fibrillin-1	*Fbn1*	−3.3
1450625_at	Procollagen V α2	*Col5a2*	−3.0
Vascular growth and patterning			
1415874_at	Sprouty homologue 1	*Spry1*	+9.0
1450414_at	Platelet-derived growth factor B	*Pdgfb*	+8.8
1425875_a_at	Leptin receptor	*Lepr*	+8.3
1460302_at	Thrombospondin-1	*Thbs1*	+5.8
1451924_at	Endothelin-1	*Edn1*	+5.3
1450922_a_at	Transforming growth factor β2	*Tgfb2*	+4.7
1416077_at	Adrenomedullin	*Adm*	+4.1
1418415_at	Homeobox B5	*Hoxb5*	+3.3
1432176_a_at	TGFβ$_1$R3 Endoglin (CD105)	*Eng*	+3.1
1435110_at	Unc 5 homologue B	*Unc5b*	+2.8
1448831_at	Angiopoietin 2	*Angpt2*	+2.8
1435458_at	Proviral integration site 1	*Pim1*	+2.6
1417455_a_at	Transforming growth factor β3	*Tgfb3*	+2.5
1438658_a_at	Endothelial differentiation sphingolipid G-protein coupled receptor 3	*Edg3*	−402
1429348_at	Semaphorin 3C	*Sema3c*	−78
1448606_a_at	Endothelial differentiation sphingolipid G-protein coupled receptor 2	*Edg2*	−72
1448925_at	Twist 2	*Twist2*	−18
1415943_at	Syndecan 1	*Sdc1*	−9.5
1427231_at	Roundabout homologue 1	*Robo1*	−5.3
1418261_at	Spleen tyrosine kinase	*Syk*	−4.9
1417011_at	Syndecan 2	*Sdc2*	−4.2
1416693_at	Forkhead box C2	*Foxc2*	−3.5
1417389_at	Glypican 1	*Gpc1*	−3.4
Miscellaneous			
1448788_at	CD200	*Cd200*	+6.0
1419728_at	ENA-78	*Cxcl5*	−62
1460227_at	Tissue inhibitor of metalloproteinase 1	*Timp1*	−7.0
1441855_x_at	GRO-α	*Cxcl1*	−6.0
1416180_a_at	Radixin	*Rdx*	−2.5

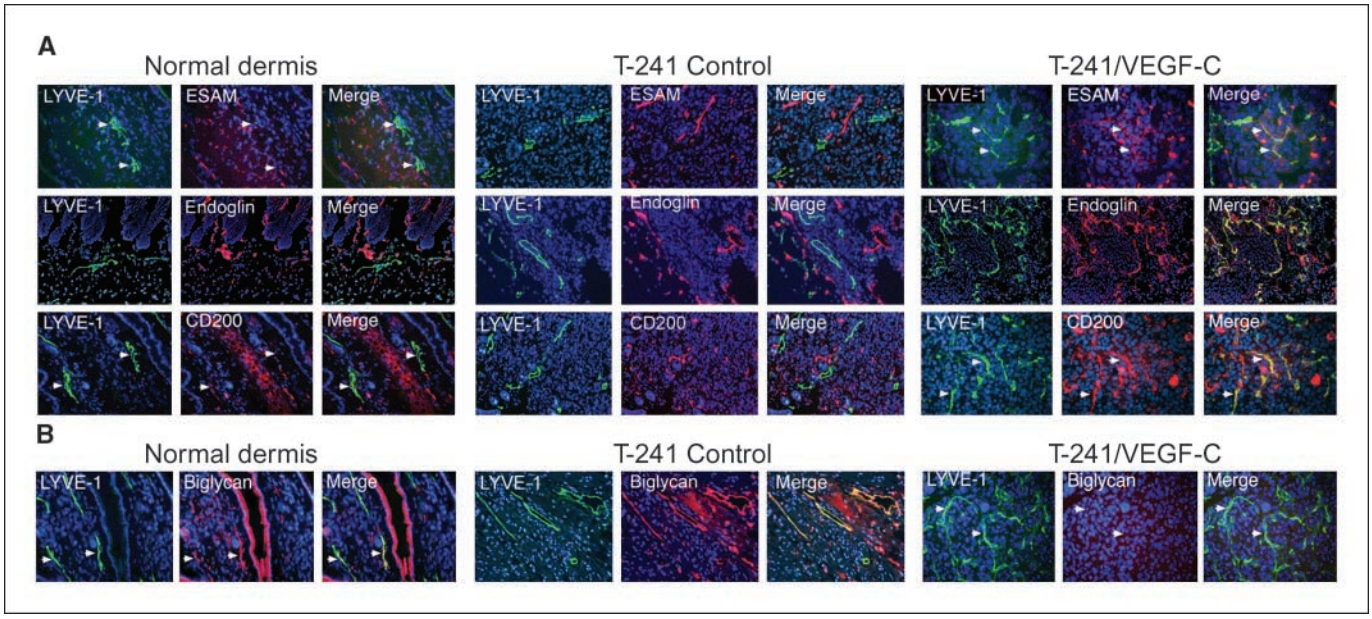

Figure 2. Confirmation of altered gene expression in lymphatics of T241/VEGF-C fibrosarcomas by comparative immunostaining. *A,* representative frozen sections of normal dermis and primary tumors from mice transplanted with either T-241 control or T-241/VEGF-C fibrosarcomas were dual immunostained for LYVE-1 (Alexa 488; *green*) and ESAM, Endoglin, or CD200 (Alexa 568; *red*) to confirm the up-regulated gene expression seen in Affymetrix microarray analyses of isolated LEC (Fig. 1*C*). ESAM, Endoglin, and CD200 expression is restricted to LYVE-1–negative blood capillaries in normal skin and nonmetastatic control T-241 tumors but selectively up-regulated in intratumoral/peritumoral LYVE-1–positive lymphatic capillaries in metastatic T-241/VEGF-C fibrosarcomas (original magnification, ×20). *B,* dual immunostaining for LYVE-1 and biglycan shows that the proteoglycan is abundant in the subendothelial matrix of LYVE-1–negative blood vessels and small LYVE-1–positive lymphatic capillaries in normal dermis and control nonmetastatic T-241 tumors but is absent from LYVE-1–positive lymphatics in metastatic T241/VEGF-C fibrosarcomas (original magnification, ×20). Arrowheads in selected images are included as points of reference for appropriate single or dual stained lymphatic capillaries.

lymphatic vessels during normal immune trafficking (20, 26, 27), their induction in tumor lymphatics may well have functional significance for invasion by metastasizing T-241/VEGF-C tumor cells. Other notable changes included down-regulation of the adherens junction proteins N-cadherin (*Cdh2*) and cadherin-11 (*Cdh11*; see Table 1). Curiously, tumor LEC also showed up-regulation of RNA for CD200, an immunoglobulin superfamily receptor reported to inhibit immune activation through binding of its receptor CD200R on myeloid cells (28). Immunostaining for ESAM and CD200 confirmed that both proteins were indeed present in LYVE-1–positive lymphatics within T-241/VEGF-C fibrosarcomas whereas neither was detected in lymphatics within normal mouse dermis (Fig. 2*A*). Moreover, neither protein was detected within the lymphatics of control T-241 fibrosarcomas lacking VEGF-C, which grow as localized nondisseminating tumors (18), consistent with an association between marker expression and nodal metastasis.

Down-regulation of subendothelial matrix proteins. A number of genes encoding key components of the extracellular matrix were differentially expressed in T-241/VEGF-C tumor-associated LEC. For example, transcripts for individual α chains of the fibrillar collagens, procollagens Iα2, IIIα1, and Vα2, and all three α-chain subunits of the network-forming fibril-associated collagen (procollagen VI) were down-regulated. We also noted down-regulation of transcripts encoding the procollagen-C endopeptidase enhancer proteins, lysyl oxidase and the small proteoglycan biglycan, which control the mechanical properties of collagen fibrils (29), and reduced expression of RNA encoding the lymphatic vessel anchoring filament protein fibrillin-1, together with the microfibril-associated proteins EMILIN-2 and Latent TGF Binding Proteins (30). In contrast, there was up-regulation of tenascin-C, a modulator of matrix adhesion commonly found in the tumor stroma and associated with promotion of tumor growth (31). We confirmed down-regulation of biglycan by immunofluorescence microscopy, which showed that the protein was present within LYVE-1–positive lymphatic vessels of normal skin and control nonmetastasizing T-241 tumors, but absent from lymphatics of nodal metastasizing T-241/VEGF-C fibrosarcomas (Fig. 2*B*). These changes in extracellular matrix and associated components suggest a possible alteration in the interaction between tumor lymphatics and the underlying fibrosarcoma matrix that may have consequences for metastasis.

Changes in molecules related to vessel growth and patterning. Several genes associated with endothelial cell proliferation and vessel sprouting were significantly up-regulated in T-241/VEGF-C tumor LEC. These included the obesity-related leptin receptor (Ob-R), a regulator of hemangiogenesis and vascular permeability (32); platelet-derived growth factor B, a form of the smooth muscle growth factor with mitogenic activity for lymphatic vessels; TGFβ2; TGFβ3; and the endothelial specific TGFβ1/3, coreceptor Endoglin/CD105 (33). We confirmed up-regulation of Endoglin by immunostaining of frozen tissue, which showed that the protein was present in LYVE-1–positive lymphatics of nodal metastasizing T-241/VEGF-C tumors but absent from those of control T-241 tumors and normal dermis (Fig. 2*A*). Differentially expressed genes implicated in vessel patterning included angiopoietin-2, a growth factor required for lymphatic vessel patterning (34); FoxC2, the transcription factor whose mutation leads to lymphatic vessel arterialization in lymphoedema distichiasis (35); Syk, a tyrosine kinase associated with blood and lymphatic vascular specification (36); and the G-protein–coupled endothelial lysophospholipid/sphingosine phosphate receptors *edg2* (LPA1) and

edg3 (S1P3). Changes in expression of the *edg* receptor family are particularly interesting because these molecules, which function on both leukocytes and endothelial cells, are known to regulate transmigration across both afferent and efferent lymphatics (37, 38).

Minimal effects of VEGF-C on lymphatic phenotype. Given that the lymph node metastasizing variant of the T-241 tumor cell line used in our study overexpresses VEGF-C, we considered the obvious possibility that the distinct expression pattern observed for tumor LEC might have resulted from direct mitogenic effects of this growth factor rather than the influence of tumor/host environment. Culture of normal murine primary dermal LEC with VEGF-C failed to induce a profile similar to T-241/VEGF-C fibrosarcoma–derived LEC when assessed by Affymetrix array analysis (not shown); however, this may be an artifact due to the low proliferation of murine LEC in response to VEGF-C *in vitro* observed by ourselves and reported by others (see ref. 39 and data not shown). Nevertheless, comparison of the T241/VEGF-C LEC profile with that of VEGF-C–treated human dermal LEC, which do proliferate in response to the growth factor (40), showed little or no overlap (not shown). Lastly, *in vivo* lymphangiogenesis studies in mice using VEGF-C-impregnated Matrigel implants revealed no induction of ESAM or CD200 within nascent lymphatics (data not shown). Hence, we conclude that the expression profile of T-241/VEGF-C tumor LEC is not simply the result of VEGF-C signaling or mitogenesis but rather a consequence of more complex effects of tumor-endothelial or stromal cell-endothelial interactions.

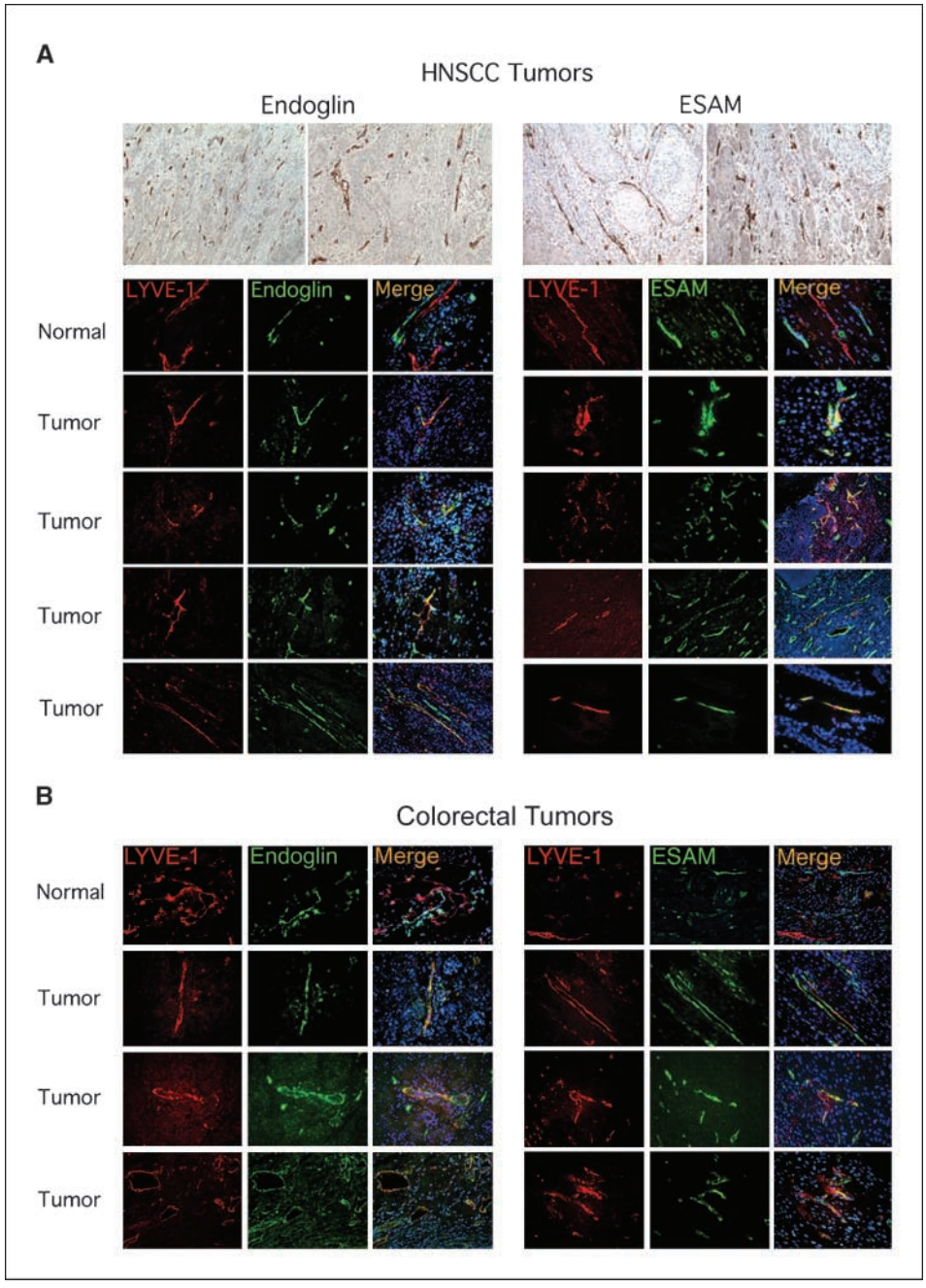

Figure 3. Immunostaining for Endoglin and ESAM in human cancer lymphatics. *A,* representative sections of HNSCC stained for Endoglin or ESAM by an immunoperoxidase method to reveal extensive expression in tumor microvasculature (*top*; original magnification, ×10 and ×20, respectively) or dual immunostained for LYVE-1/Alexa 568 (*red*) and either Endoglin or ESAM/Streptavidin Alexa 488 (*green*) to show expression in intratumoral and peritumoral tissue compared with normal marginal tissue (*bottom*; original magnification, ×20). Merged images include DAPI staining. *B,* representative sections of colorectal carcinomas and normal marginal tissue dual immunostained for LYVE-1/Alexa 568 (*red*) and either Endoglin or ESAM/Streptavidin Alexa 488 (*green*). Merged images include DAPI staining. Original magnification, ×20.

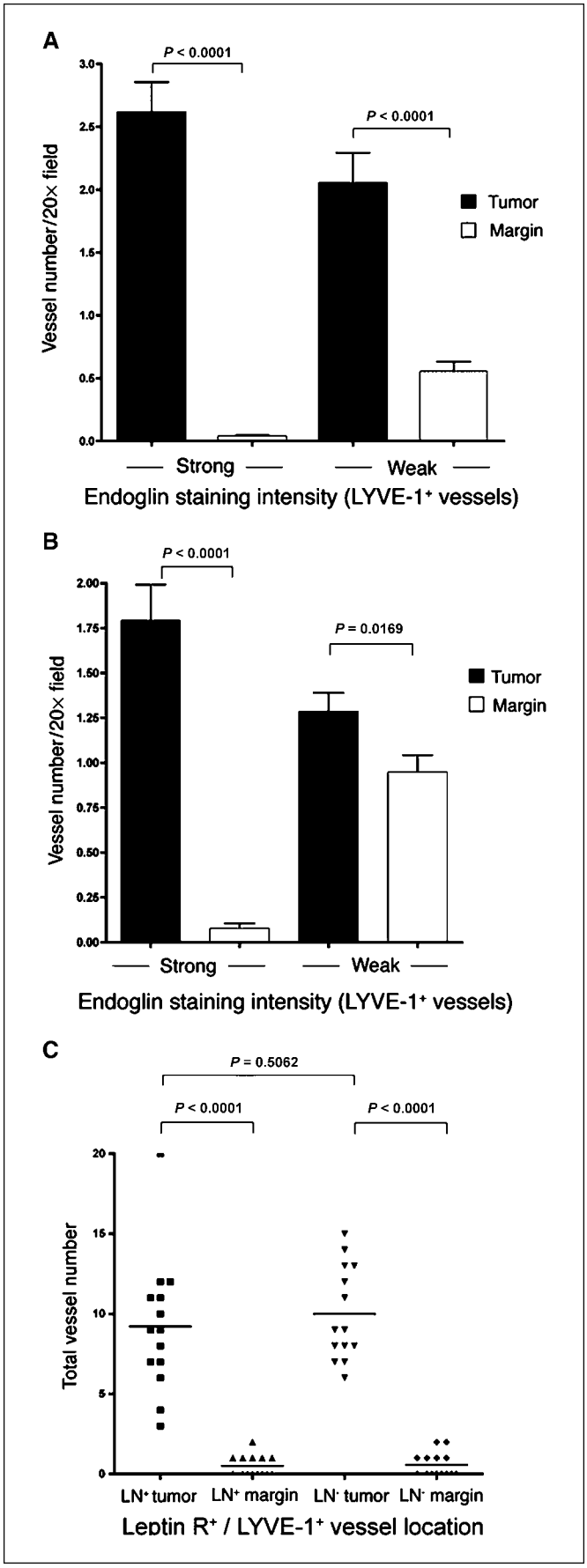

Figure 4. Quantitative analysis of Endoglin- and leptin-R–positive lymphatics in HNSCC and colorectal carcinoma. Bar charts show counts for Endoglin-positive lymphatic vessel numbers present within the tumor and normal margin in 28 cases each of HNSCC (*A*) and colorectal carcinoma (*B*) assessed by dual LYVE-1 immunofluorescence microscopy. Endoglin expression is scored as either strong or weak according to staining intensity (see Materials and Methods). A scatter plot (*C*) shows individual counts for total leptin-R–positive lymphatic vessel numbers in tumor and normal margin of the same HNSCC series (see Materials and Methods), including comparison between cases with (LN^+) or without (LN^-) lymph node metastases. *Columns,* mean; *bars,* SE.

Confirmation of an altered phenotype for tumor lymphatics in human cancers. We next determined how far the lymphatic phenotype observed in the mouse fibrosarcoma model might extend to naturally occurring human cancers, and how any observed changes in the expression of candidate genes might relate to nodal metastasis. In initial studies we detected both ESAM and Endoglin immunostaining specifically in tumor lymphatics, but not normal marginal lymphatics, within a range of different cancers including melanoma and lung, ovarian, breast, endometrial, and hepatocellular carcinomas (Supplementary Fig. S3 and data not shown). Importantly, we confirmed the authenticity of both ESAM- and Endoglin-positive vessels as lymphatics in these human cancer tissues by two- and three-color immunostaining with LYVE-1 and either podoplanin or PROX-1 (Supplementary Figs. S4, S6, and S7), discounting the possibility that they represented infiltrating LYVE-1–positive macrophages or blood vessels.

For more extensive analyses, we assembled panels of paraffin-embedded tumor tissues from 28 patients with primary HNSCC (5, 41) and 28 with primary colorectal carcinoma. Both series included equal numbers of cases with or without demonstrable lymph node metastasis. Focusing on ESAM, Endoglin/CD105, and the hemangiogenesis-associated leptin-R (Ob-R; ref. 32), due to poor reactivity of antibodies to such additional markers as Coxsackie adenovirus receptor and CD200 in paraffin sections, we compared expression on LYVE-1–positive lymphatics in tumors and LYVE-1–positive lymphatics within normal marginal tissues by dual immunofluorescent antibody staining. As shown by the fluorescence micrographs in Fig. 3 and Supplementary Fig. S5, Endoglin, ESAM, and leptin-R were detected in numerous LYVE-1–positive tumor lymphatics in both HNSCC and colorectal carcinomas. In addition, some positive staining could be seen in LYVE-1–negative vessels (data not shown), consistent with known expression of these receptors in normal and neoplastic hemovascular endothelium (20, 42, 43). However, in lymphatics, all three markers were strongly expressed in peritumoral and, in some cases, intratumoral vessels, whereas only weak expression was seen in normal stromal vessels.

Quantitative analysis of immunostained vessels confirmed these initial observations and revealed a striking association between Endoglin-positive vessel incidence and tumor location among lymphatics in both HNSCC (Fig. 4*A*) and colorectal carcinomas (Fig. 4*B*), particularly among strongly Endoglin-positive vessels (2.61 ± 0.24 vessels per field in HNSCC tumor versus 0.02 ± 0.01 in marginal tissue, $P < 0.0001$; 1.79 ± 0.2 vessels per field in colorectal tumor versus 0.08 ± 0.03 in marginal tissue, $P < 0.0001$), although this was less obvious among more weakly stained vessels. Interestingly, there was also a significant association between tumor Endoglin-positive vessel number and the presence of lymph node metastases in HNSCC (Supplementary Fig. S8), although once again this was less marked among weakly stained vessels. A clear association between marker induction and neoplasia was also

apparent from similar analyses of leptin-R within the lymphatics in HNSCC (9.61 ± 0.68 vessels per field in tumor versus 0.54 ± 0.13 in marginal tissue, $P < 0.0001$), although in this case there was no obvious association with nodal metastasis (Fig. 4*C*).

Finally, a quantitative analysis of lymphatic vessel ESAM staining confirmed similarly substantial up-regulation of this protein on tumor vessels in both HNSCC and colorectal carcinoma (Fig. 5*A* and *B*). Most notably, however, there was a dramatic association between the incidence of ESAM-positive tumor vessels and the presence of lymph node metastases (17.9 ± 2.66 vessels per field in node-positive HNSCC versus 0.57 ± 0.27 in node-negative HNSCC, $P < 0.0001$; 7.07 ± 1.34 vessels per field in node-positive colorectal tumors versus 1.36 ± 0.37 in node-negative colorectal tumors, $P = 0.0002$).

In summary, our data provide clear confirmation that several of the tumor lymphatic markers we identified in experimental murine T-241/VEGF-C fibrosarcoma are also up-regulated in human cancers. Moreover, they suggest that ESAM may have significant prognostic value as an indicator of tumor metastasis.

Discussion

The identification of genes selectively expressed in tumor lymphatics represents a major step toward identifying biomarkers for metastasis and for elucidating the mechanisms by which tumors invade the microvasculature and spread to lymph nodes. In the foregoing analyses, we identified some 792 transcripts with significantly altered expression, a difference of the same order as that found in recent comparisons of lymphatic and blood endothelial cells from human dermis (44, 45). It is thus evident that an interplay between lymphatic vessels and the tumor environment can have a more significant effect on endothelial phenotype than might have been anticipated. Surprisingly, such effects could not be attributed to the direct action of VEGF-C as adduced by comparisons with the RNA profile of dermal LEC stimulated with the growth factor (40). Perhaps the low responsiveness of adult lymphatics to both VEGF-C and VEGF-D compared with embryonic and neonatal lymphatics may help explain this finding (46). We also note that conditions of acute inflammation that stimulate the exit of leukocytes from tissue to lymph induce none of the genes up-regulated in tumor LEC (19). Hence, tumors may not necessarily exploit the tactics of the immune system for spread to the lymph nodes.

Although the present array analyses were confined largely to murine fibrosarcoma lymphatics, the fact that we could validate these findings for three key markers, Endoglin, ESAM, and leptin-R, in human cancers is an indication that the alterations in LEC transcriptional profile underlie fundamental processes that cross species barriers—a property shared by tumor blood endothelial markers originally identified in Sequential Analysis of Gene Expression analyses of human cancers (47). It is interesting to note that ESAM, the closely related JAM-A and JAM-C (VE-JAM), and Coxsackie adenovirus receptor have all been shown to function as homophilic or heterophilic tight junction adhesion molecules in different contexts (see ref. 48). In particular, ESAM has been shown to mediate transendothelial migration of neutrophils through signaling via the small GTP-binding protein Rho that is implicated in the destabilization of tight junctions (20), whereas ESAM knockout mice show defective tumor angiogenesis. It is tempting to speculate that ESAM could mediate the lymphatic entry of tumor cells and subsequent nodal metastasis. The recent availability of ESAM$^{-/-}$ mice (20) will allow this hypothesis to be tested in the future.

It is likewise interesting that Endoglin, a component of the transforming growth factor (TGFβ) receptor complex associated with hemangiogenesis (49), is a well-known marker of proliferating tumor blood vessels. Indeed, it is an independent predictor of metastasis with potential value in diagnostic imaging and therapeutic targeting (50). The up-regulated expression in tumor lymphatics observed here clearly indicates that Endoglin is not confined to the blood vasculature, although the relative

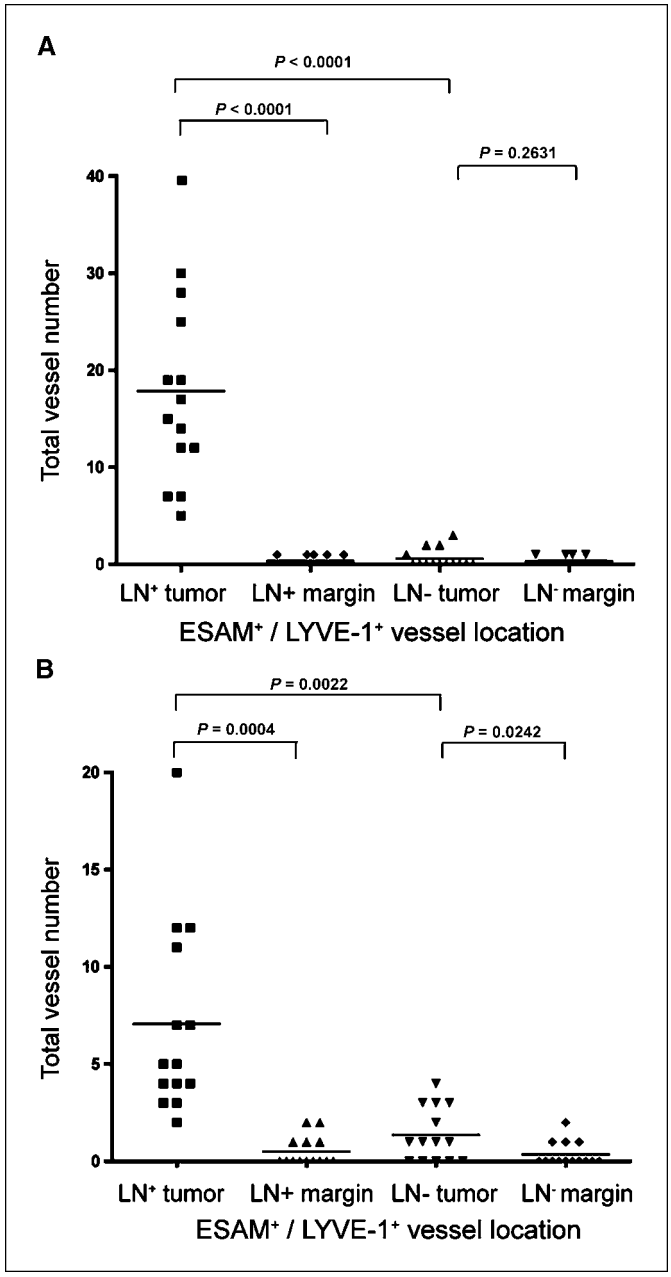

Figure 5. Association between ESAM-positive lymphatic vessel number and lymph node metastasis in HNSCC and colorectal carcinoma. Scatter plots show individual counts for total ESAM-positive lymphatic vessel numbers (see Materials and Methods) present within the tumor and normal margin in 28 cases each of HNSCC (*A*) and colorectal carcinomas (*B*) categorized according to the presence or absence of demonstrable lymph node metastases, assessed by dual LYVE-1 immunofluorescence microscopy. *Points,* mean; *bars,* SE.

heterogeneity in expression of the receptor in tumor lymphatics may complicate its use as a prognostic marker by comparison with ESAM. Such findings signal the need for further investigation into the role of Endoglin in lymphangiogenesis as well as caution in its use as a marker for immunoisolation of blood vessel endothelium (17).

Finally, the further validation of our array data through comprehensive screening of normal and pathologic tissues may well identify robust new tumor-specific lymphatic markers for both prognosis and therapy. Indeed, in this article, we have already identified one such candidate, ESAM, whose expression is strongly associated with lymph node metastasis in HNSCC and colorectal carcinoma. There is considerable need for such markers in assessing treatment strategies for cancer patients at the early stages of disease, where alteration in vessel properties may signal metastasis. Most previous studies seeking to correlate levels of lymphangiogenic growth factors and lymphatic vessel density with nodal metastasis and patient survival have made the assumption that tumor spread is limited primarily by the number, rather than the nature, of lymphatic capillaries present within the primary tumor mass (51–54). More often than not, such studies have yielded conflicting results. The findings reported here highlight the importance of qualitative changes in the tumor lymphatics and lay the foundations for developing novel lymphatic markers that accurately assess metastatic potential and enlighten future therapies.

Disclosure of Potential Conflicts of Interest

No potential conflicts of interest were disclosed.

Acknowledgments

Received 12/4/2007; revised 6/16/2008; accepted 6/30/2008.

Grant support: Cancer Research UK grant C581 (D.G. Jackson), National Coordinating Centre for Research Capacity Development Research Fellowship scheme (D. Royston), Deutsche Forschungsgemeinschaft grant SFB492 and European Community grant NoE MAIN 502935 (D. Vestweber), and grants from the Swedish Cancer Foundation and Karolinska Research Foundation (Y. Cao).

The costs of publication of this article were defrayed in part by the payment of page charges. This article must therefore be hereby marked *advertisement* in accordance with 18 U.S.C. Section 1734 solely to indicate this fact.

References

1. Achen M, Mann GB, Stacker S. Targeting lymphangiogenesis to prevent tumour metastasis. Br J Cancer 2006; 94:1355–60.
2. Witte MH, Jones K, Wilting J, et al. Structure-function relationships in the lymphatic system and implications for cancer biology. Cancer Metastasis Rev 2006;25:159–84.
3. Ley K, Laudanna C, Cybulsky MI, Nourshargh S. Getting to the site of inflammation: the leukocyte adhesion cascade updated. Nat Rev Immunol 2007;7: 678–89.
4. Shields J, Emmett MS, Dunn DBA, et al. Chemokine-mediated migration of melanoma cells towards lymphatics—a mechanism contributing to metastasis. Oncogene 2006;26:2997–3005.
5. Beasley NJ, Prevo R, Banerji S, et al. Intratumoral lymphangiogenesis and lymph node metastasis in head and neck cancer. Cancer Res 2002;62:1315–20.
6. Stacker SA, Achen MG, Jussila L, Baldwin ME, Alitalo K. Lymphangiogenesis and cancer metastasis. Nat Rev Cancer 2002;2:573–83.
7. Skobe M, Hawighorst T, Jackson DG, et al. Induction of tumor lymphangiogenesis by VEGF-C promotes breast cancer metastasis. Nat Med 2001;7:192–8.
8. Mandriota SJ, Jussila L, Jeltsch M, et al. Vascular endothelial growth factor-C-mediated lymphangiogenesis promotes tumour metastasis. EMBO J 2001;20: 672–82.
9. Stacker SA, Caesar C, Baldwin ME, et al. VEGF-D promotes the metastatic spread of tumor cells via the lymphatics. Nat Med 2001;7:186–91.
10. Hoshida T, Isaka N, Hagendoorn J, et al. Imaging steps of lymphatic metastasis reveals that vascular endothelial growth factor-C increases metastasis by increasing delivery of cancer cells to lymph nodes: therapeutic implications. Cancer Res 2006;66:8065–75.
11. Zhang L, Giraudo E, Hoffman JA, Hanahan D, Ruoslahti E. Lymphatic zip codes in premalignant lesions and tumors. Cancer Res 2006;66:5696–706.
12. Breslin JW, Gaudreault N, Watson KD, Reynoso R, Yuan S, Wu, MH. Vascular endothelial growth factor-C stimulates the lymphatic pump by a VEGF receptor-3-dependent mechanism. Am J Physiol Heart Circ Physiol 2007;293:709–18.
13. Eichten A, Hyun WC, Coussens LM. Distinctive features of angiogenesis and lymphangiogenesis determine their functionality during *de novo* tumor development. Cancer Res 2007;67:5211–20.
14. St Croix B, Rago C, Velculescu V, et al. Genes expressed in human tumor endothelium. Science 2000; 289:1197–202.
15. Nanda A, Buckhaults P, Seaman S, et al. Identification of a binding partner for the endothelial cell surface proteins TEM7 and TEM7R. Cancer Res 2004;64:8507–11.
16. Nanda A, Carson-Walter EB, Seaman S, et al. TEM8 interacts with the cleaved C5 domain of collagen α 3(VI). Cancer Res 2004;64:817–20.
17. Seaman S, Stevens J, Yang MY, Logsdon D, Graff-Cherry C, St. Croix B. Genes that distinguish physiological and pathological angiogenesis. Cancer Cell 2007;11: 539–54.
18. Cao R, Bjorndahl MA, Religa P, et al. PDGF-BB induces intratumoral lymphangiogenesis and promotes lymphatic metastasis. Cancer Cell 2004;6:333–45.
19. Johnson LA, Clasper S, Holt A, Lalor P, Baban D, Jackson DG. An inflammation-induced mechanism for leukocyte transmigration of lymphatic endothelium. J Exp Med 2006;203:2763–77.
20. Wegmann F, Petri B, Khandoga AG, et al. ESAM supports neutrophil extavsation, activation of Rho, and VEGF-induced vascular permeability. J Exp Med 2006; 203:1671–7.
21. Brazma A, Hingamp P, Quackenbush J, et al. Minimum information about a microarray experiment (MIAME)—towards standards for microarray data. Nat Genet 2001;29:365–71.
22. Bolstad BM, Irizarry RA, Astrand M, Speed TPA. Comparison of normalization methods for high density oligonucleotide array data based on bias and variance. Bioinformatics 2003;19:185–93.
23. Irizarry RA, Hobbs B, Collin F, et al. Exploration, normalization, and summaries of high density oligonucleotide array probe level data. Biostatistics 2003;4: 249–64.
24. Wang X, Seed B. A PCR primer bank for quantitative gene expression analysis. Nucleic Acids Res 2003;31: e154.
25. Johnson LA, Prevo R, Clasper S, Jackson DG. Inflammation-induced uptake and degradation of the lymphatic endothelial hyaluronan receptor LYVE-1. J Biol Chem 2007;282:33671–80.
26. Cera MR, Del Prete A, Vecchi A, et al. Increased DC trafficking to lymph nodes and contact hypersensitivity in junctional adhesion molecule-A-deficient mice. J Clin Invest 2004;114:729–38.
27. Zen K, Liu Y, McCall IC, et al. Neutrophil migration across tight junctions is mediated by adhesive interactions between epithelial coxsackie and adenovirus receptor and a junctional adhesion molecule-like protein on neutrophils. Mol Biol Cell 2005;16:2694–703.
28. Nathan C, Muller WA. Putting the brakes on innate immunity: a regulatory role for CD200? Nat Immunol 2001;2:17–9.
29. Schonherr E, Witsch-Prehm P, Harrach B, Robenek H, Rauterberg J, Kresse H. Interaction of biglycan with type I collagen. J Biol Chem 1995;270:2776–83.
30. Isogai Z, Ono RN, Ushiro S, et al. Latent transforming growth factor β-binding protein 1 interacts with fibrillin and is a microfibril-associated protein. J Biol Chem 2003;278:2750–7.
31. Tanaka K, Hiraiwa N, Hashimoto H, Yamazaki Y, Kusakabe M. Tenascin-C regulates angiogenesis in tumor through the regulation of vascular endothelial growth factor expression. Int J Cancer 2004;108:31–40.
32. Cao R, Brakenhielm E, Wahlestedt C, Thyberg J, Cao Y. Leptin induces vascular permeability and synergistically stimulates angiogenesis with FGF-2 and VEGF. Proc Natl Acad Sci U S A 2001;98:6390–5.
33. Lebrin F, Deckers M, Bertolino P, Ten Dijke P. TGF-β receptor function in the endothelium. Cardiovasc Res 2005;65:599–608.
34. Gale NW, Thurston G, Hackett SF, et al. Angiopoietin-2 is required for postnatal angiogenesis and lymphatic patterning, and only the latter role is rescued by angiopoietin-1. Dev Cell 2002;3:411–23.
35. Finegold DN, Kimak MA, Lawrence EC, et al. Truncating mutations in FOXC2 cause multiple lymphedema syndromes. Hum Mol Genet 2001;10:1185–9.
36. Abtahian F, Guerriero A, Sebzda E, et al. Regulation of blood and lymphatic vascular separation by signaling proteins SLP-76 and Syk. Science 2003;299:247–51.
37. Matloubian M, Lo CG, Cinamon G, et al. Nature 2004; 427:355–60.
38. Ledgerwood LG, Lal G, Zhang N, et al. The sphingosine 1-phosphate receptor 1 causes tissue retention by inhibiting the entry of peripheral tissue T lymphocytes into afferent lymphatics. Nat Immunol 2007;9:42–53.
39. Schacht V, Ramirez MI, Hong YK, et al. T1 α/podoplanin deficiency disrupts normal lymphatic vasculature formation and causes lymphedema. EMBO J 2003;22:3546–56.
40. Yong C, Bridenbaugh EA, Zawieja D, Swartz MA. Microarray analysis of VEGF-C responsive genes in human lymphatic endothelial cells. Lymphat Res Biol 2005;3:183–207.
41. Maula SM, Luukkaa M, Grenman R, Jackson D, Jalkanen S, Ristamaki R. Intratumoral lymphatics are essential for the metastatic spread and prognosis in squamous cell carcinomas of the head and neck region. Cancer Res 2003;63:1920–6.

42. Hirata K, Ishida T, Penta K, et al. Cloning of an immunoglobulin family adhesion molecule selectively expressed by endothelial cells. J Biol Chem 2001;276:16223–31.

43. Ishida T, Kundu RK, Yang E, Hirata K, Ho YD, Quertermous T. Targeted disruption of endothelial cell-selective adhesion molecule inhibits angiogenic processes *in vitro* and *in vivo*. J Biol Chem 2003;278:34598–604.

44. Podgrabinska S, Braun P, Velasco P, et al. Molecular characterization of lymphatic endothelial cells. Proc Natl Acad Sci USA 2002;99:16069–74.

45. Hirakawa S, Hong YK, Harvey N, et al. Identification of vascular lineage-specific genes by transcriptional profiling of isolated blood vascular and lymphatic endothelial cells. Am J Pathol 2003;162:575–86.

46. Karpanen T, Wirzenius M, Makinen T, et al. Lymphangiogenic growth factor responsiveness is modulated by postnatal lymphatic vessel maturation. Am J Pathol 2006;169:708–18.

47. Carson-Walter EB, Watkins DN, Nanda A, Vogelstein B, Kinzler K, St Croix B. Cell surface tumor endothelial markers are conserved in mice and humans. Cancer Res 2001;61:6649–55.

48. Ebnet K, Suzuki A, Ohno S, Vestweber D. Junctional adhesion molecules (JAMs): more molecules with dual functions? J Cell Sci 2004;117:19–29.

49. Li DY, Sorensen LK, Brooke BS, et al. Defective angiogenesis in mice lacking Endoglin. Science 1999;284:1534–7.

50. Fonsatti E, Maio M. Highlights on Endoglin (CD105): from basic findings towards clinical applications in human cancer. J Transl Med 2004;2:18–24.

51. Nathanson SD, Zarbo RJ, Wachna DL, Spence CA, Andrzejewski TA, Abrams J. Microvessels that predict axillary lymph node metastases in patients with breast cancer. Arch Surg 2000;135:586–93.

52. Bono P, Wasenius V, Lundin J, Jackson DG, Joensuu H. High peritumoral LYVE-1 positive lymphatic vessel numbers are associated with axillary lymph node metastases and poor outcome in early breast cancer. Clin Cancer Res 2004;10:7144–9.

53. Shields JD, Borsetti M, Rigby H, et al. Lymphatic density and metastatic spread in human malignant melanoma. Br J Cancer 2004;90:693–700.

54. Von Marschall Z, Scholz A, Stacker S, et al. Vascular endothelial growth factor-D induces lymphangiogenesis and lymphatic metastasis in models of ductal pancreatic cancer. Int J Oncol 2005;27:669–79.